# Fundamental measure theory for mixtures of parallel hard cubes. II. Phase behavior of the one-component fluid and of the binary mixture

Yuri Martínez-Ratón[a] and José A. Cuesta[b]

*Grupo Interdisciplinar de Sistemas Complicados (GISC), Departamento de Matemáticas, Universidad Carlos III de Madrid, Avda. de la Universidad, 30, 28911-Leganés, Madrid, Spain*

A previously developed fundamental measure functional [J. Chem. Phys. **107**, 6379 (1997)] is used to study the phase behavior of a system of parallel hard cubes. The single-component fluid exhibits a continuous transition to a solid with an anomalously large density of vacancies. The binary mixture has a demixing transition for edge–length ratios below 0.1. Freezing in this mixture reveals that at least the phase rich in large cubes always lies in the region where the uniform fluid is unstable, hence suggesting a fluid–solid phase separation. A method is developed to study very asymmetric binary mixtures by taking the limit of zero size ratio at fixed solvent fugacity. With this procedure the mixture is exactly mapped onto a one-component fluid of parallel adhesive hard cubes. At any density and solvent fugacity the large cubes are shown to collapse into a close-packed solid. Nevertheless the phase diagram contains a large metastability region with fluid and solid phases. Upon introduction of a slight polydispersity in the large cubes, the system shows the typical phase diagram of a fluid with an isostructural solid–solid transition (with the exception of a continuous freezing). Consequences about the phase behavior of binary mixtures of hard core particles are then drawn. © *1999 American Institute of Physics.* [S0021-9606(99)52024-2]

## I. INTRODUCTION

This paper is the sequel of a previous one[1] (henceforth referred to as I) in which the so-called *fundamental measure theory* (FMT) was applied to build a density functional for the multicomponent system of parallel hard cubes (PHC). In I we explained all fundamentals of the theory and gave a full account of the technical details involved in the derivation of the functional. We also discussed the pros and cons of the theory, as compared with more standard density functional theories (DFTs), and suggested some possible extensions.

In this paper we apply the formalism developed in I to study the phase behavior of the PHC fluid, with special emphasis in its relevance for the understanding of the phase behavior of mixtures. The PHC fluid is a rather academic model and it possesses a bunch of "peculiarities" which are rather odd for a fluid model, e.g., the uniform fluid is anisotropic at small scales (the cubes are kept parallel to each other), freezing occurs at very low packing fractions (around 0.3–0.4), and it is a continuous, instead of first order, transition (a consequence of the lack of isotropy of the fluid phase), and the depletion in the binary mixture is very strong compared to hard spheres (HS). But in spite of these peculiarities, which certainly make of this model a caricature of a fluid, the physics one can learn from its phase behavior can be easily extended to more reasonable fluids, and it has the important added value of being a much simpler model to carry out analytical calculations (even more: FMT seems to be somehow optimal for this model).[1,2]

There have been a few previous studies in the literature about the fluid of PHC[3–8] scattered in the last forty years, but the relevance of this model has only recently become apparent when it has been proposed as a model of a fluid able to demix by a purely entropic mechanism.[9,10]

Entropic demixing has been a long standing question which only recently begins to be understood. It is well known that different attractions between two types of particles in a fluid can produce segregation into two phases, each rich in one type of particles.[11] The question remains whether hard particles, for which only an entropic balance can drive a phase transition, ever demix and how. It is clear that nonadditive mixtures (mixtures in which particles of different types interact as if they had a larger volume) do demix,[12–15] but they have the segregation mechanism introduced at the interaction potential. So the nontrivial question concerns additive hard-particle mixtures. The question is tricky because the simplest model of this type, HS, was solved in Percus–Yevick (PY) approximation[16] and shown never to demix.[17] It had to wait almost thirty years until the PY result was questioned. By solving numerically the Ornstein–Zernike equation with closure relations more accurate than the PY one, a spinodal instability was shown to occur in a binary mixture of HS[18–20] for a diameter ratio below 0.1–0.25 (depending of the authors).

It was then believed that a sufficiently asymmetric HS binary mixture undergoes fluid–fluid demixing in a certain region of the phase diagram. But successive experiments performed in suspensions of polystyrene or silica spheres (which to a large accuracy can be considered HS) showed cumulative evidence that demixing is coupled to freezing, and so one of the phases shows up as a crystal, sometimes a

[a]Electronic mail: yuri@alum.math.uc3m.es
[b]Electronic mail: cuesta@math.uc3m.es

glass, of large particles.[21–24] Recent theoretical calculations confirm this scheme.[25,26]

Direct computer simulations have run into trouble when dealing with this problem due to the extremely low probability of moving a large particle in a sea of small ones without overlapping any of them. Simulations are still possible for not too dissimilar diameters, but they do not show demixing.[27,28] With the help of specially designed cluster moves, the first evidence of demixing has recently been found in simulations for diameter ratios smaller than 0.05.[29] Unfortunately these cluster moves do not help above the percolation threshold, and this sets a relatively low upper bound for the total packing fraction of the fluid. Besides, this method does not allow the identification of the coexisting phases, so it does not distinguish fluid–fluid or fluid–solid demixing.

In order to elucidate the nature of demixing for very asymmetric mixtures the attention has shifted to understand the depletion interaction. An effective pair potential between the large spheres can be obtained by different procedures.[30–33] Its shape reveals a very deep and narrow (one small-sphere diameter) well followed by a couple of small oscillations extending two or three small-sphere diameters. The depth and the amplitude of the oscillations depend on the small spheres packing fraction. In view of the phase behavior of spheres with narrow and deep attractive potentials,[34,35] fluid–fluid demixing is ruled out for sufficient asymmetry, and instead fluid–solid demixing or even expanded–dense solid demixing (i.e., demixing once the large component has crystallized) should appear. Simulations of a system of HS supplemented by the depletion potential[31–33] confirm this conjecture if the diameter ratio is below 0.1. Expanded–dense solid demixing is indeed shown in some of these simulations for ratios 0.1 (Ref. 32) or 0.05.[33] This phase behavior has been recently corroborated by *direct* simulations of the binary mixture,[36] which have been shown to be possible in the relevant region of the phase diagram thanks to the small amount of small spheres present in those statepoints.

In the limit of zero size of the small spheres at constant packing fraction the depletion potential becomes Baxter's adhesive potential.[37,38] By applying a similar limit to the FMT functional of a binary mixture of PHC[1,2] we have recently obtained a functional for parallel adhesive hard cubes (PAHC).[39] By avoiding the singularities of this potential (we will treat this point in detail later on) we show that the phase behavior of this fluid is consistent with the above described picture for the mixture of HS, with the difference that expanded–dense solid demixing is the most common scenario because PAHC freezing occurs at rather low packing fractions.

## II. THE ONE-COMPONENT FLUID

There are relatively few results in the literature concerning the fluid of PHC. As concerns the uniform fluid the virial coefficients, both in 2D and 3D, have been exactly obtained through diagrammatic expansions up to the seventh.[3,4] They have also been obtained for different approximate integral equation theories.[5] The main consequence one draws from
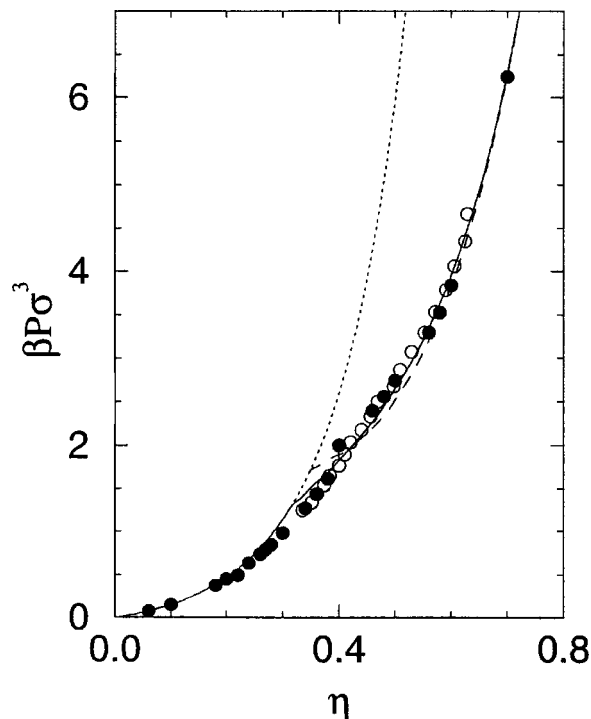


FIG. 1. Equation of state of the PHC fluid. Solid lines correspond to the pressure of the stable phase (fluid or solid) at the given packing fraction, $\eta$. Dotted line is the unstable fluid branch beyond freezing. Dashed line is the solid branch computed without accounting for vacancies in the lattice (see text). Full circles are the simulations of Ref. 6 and empty circles those of Ref. 7 (actually we have averaged the two data sets reported for the largest system size).

this information is that the virial expansion is very poorly convergent. For the 3D fluid, the seventh order virial expansion exhibits a maximum in the pressure at $\eta \approx 0.6$, and then goes down very quickly to reach negative values.[5] Its behavior at moderate densities strongly deviates from that of a sixth-order virial expansion, in contrast to what happens for HS. This is the fingerprint of a nearby divergence. In fact, the simulations of the fluid of PHC (3D)[6,7] show a continuous freezing into a simple cubic lattice at[7] $\eta = 0.48 \pm 0.02$ (in contrast with the first order nature of the HS freezing). This result has been proven to be exact in infinite dimensions.[8] The reason for a continuous freezing is the lack of rotational symmetry of this system even in the disordered phase[8] (thus freezing does not break this symmetry). Allowing the cubes to rotate restores the first-order nature of the freezing transition.[7]

FMT's equation of state of the uniform PHC fluid is simply that of the scaled particle theory (SPT), i.e., from Eqs. (60) and (61) of I, $\beta P/\rho = 1/(1-\eta)^2$ for $D=2$ and $\beta P/\rho = (1+\eta)/(1-\eta)^3$ for $D=3$, with $\beta$ the inverse absolute temperature in Boltzmann constant units, $P$ the pressure, $\rho$ the number density, and $\eta$ the packing fraction, $\eta = \rho \sigma^D$, $\sigma$ being the cube edge-length. In Fig. 1 the SPT equation of state for $D=3$ is compared with the simulation data.

On the other hand freezing can be studied as usual in DFT by parametrizing the local density with a sum of Gaussians centered at the lattice points.[40] Since the lattice is simple cubic, this can be easily achieved by setting

$$\rho(\mathbf{r}) = s(x)s(y)s(z), \tag{1a}$$

$$s(u) \equiv \sum_{n=-\infty}^{\infty} g(u-nd), \tag{1b}$$

$$g(u) \equiv \left(\frac{\alpha}{\pi}\right)^{1/2} e^{-\alpha u^2}, \tag{1c}$$

with $d = \eta^{-1/3}\sigma$ the lattice spacing, and $\alpha$ a variational parameter determining the localization of particles at the lattice sites.

In I we expressed the free-energy functional of a multicomponent system with density profiles $\rho_i(\mathbf{r})$ ($i$ labeling the species) as $F[\{\rho_i\}] = F^{\text{id}}[\{\rho_i\}] + F^{\text{ex}}[\{\rho_i\}]$, where

$$\beta F^{\text{id}}[\{\rho_i\}] = \sum_i \int d\mathbf{r}\, \rho_i(\mathbf{r})[\ln \mathcal{V}_i\rho_i(\mathbf{r}) - 1], \tag{2}$$

$$\beta F^{\text{ex}}[\{\rho_i\}] = \int d\mathbf{r}\, \Phi(\{n_\alpha(\mathbf{r})\}), \tag{3}$$

$\mathcal{V}_i$ being the thermal volume of species $i$, and $n_\alpha = \Sigma_i \rho_i * \omega_i^{(\alpha)}$ a set of four weighted densities (star denotes convolution) defined by the weights

$$\omega_i^{(0)} \equiv \delta_i^x \delta_i^y \delta_i^z, \quad \mathbf{w}_i^{(1)} \equiv (\theta_i^x \delta_i^y \delta_i^z, \delta_i^x \theta_i^y \delta_i^z, \delta_i^x \delta_i^y \theta_i^z),$$

$$\mathbf{w}_i^{(2)} \equiv (\delta_i^x \theta_i^y \theta_i^z, \theta_i^x \delta_i^y \theta_i^z, \theta_i^x \theta_i^y \delta_i^z), \quad \omega_i^{(3)} \equiv \theta_i^x \theta_i^y \theta_i^z, \tag{4}$$

with $\theta_i^u \equiv \Theta(\sigma_i/2 - |u|)$, and $\delta_i^u \equiv (1/2)\delta(\sigma_i/2 - |u|)$. As in I we will also need the two scalar densities $n_i = n_{i,x} + n_{i,y} + n_{i,z}$, $n_{i,\nu}$, $\nu = x,y,z$, being the vector components of $\mathbf{n}_i$, $i = 1,2$. The function $\Phi(\mathbf{r})$ is given in terms of the $n_\alpha$'s as (see I)

$$\Phi(\mathbf{r}) = -n_0 \ln(1-n_3) + \frac{\mathbf{n}_1 \cdot \mathbf{n}_2}{1-n_3} + \frac{n_{2,x}n_{2,y}n_{2,z}}{(1-n_3)^2}, \tag{5}$$

with $n_{2,\nu}$, $\nu = x,y,z$, the components of $\mathbf{n}_2$.

For convenience let us introduce the functions

$$e(u) \equiv \tfrac{1}{2}\text{erf}(\sqrt{\alpha}u), \tag{6}$$

$$p(u) \equiv \sum_{n=-\infty}^{\infty} [e(u-nd+\sigma/2) - e(u-nd-\sigma/2)], \tag{7}$$

$$q(u) \equiv \sum_{n=-\infty}^{\infty} [g(u-nd+\sigma/2) + g(u-nd-\sigma/2)], \tag{8}$$

(notice that $g(u) = e'(u)$). The latter two are periodic with period $d$. In terms of these functions

$$n_3 = p(x)p(y)p(z), \tag{9a}$$

$$\mathbf{n}_2 = \tfrac{1}{2}(q(x)p(y)p(z), p(x)q(y)p(z), p(x)p(y)q(z)), \tag{9b}$$

$$\mathbf{n}_1 = \tfrac{1}{4}(p(x)q(y)q(z), q(x)p(y)q(z), q(x)q(y)p(z)), \tag{9c}$$

$$n_0 = \tfrac{1}{8}q(x)q(y)q(z), \tag{9d}$$

and accordingly $\Phi(\mathbf{r}) = n_0(\mathbf{r})\psi(\mathbf{r})$, where

$$\psi = -\ln(1-n_3) + \frac{n_3}{1-n_3} + \frac{n_3^2}{(1-n_3)^2}. \tag{10}$$

This simplification occurs because of the factorization of the density (1a), and hence of (9).

The free energy *per particle*, $\Psi \equiv \beta F/N$, of the solid phase can be obtained as the integral over a unit cell of the lattice of the free energy density. Hence the ideal part turns out to be

$$\Psi^{\text{id}} = \int_{-d/2}^{d/2} dx \int_{-d/2}^{d/2} dy \int_{-d/2}^{d/2} dz\, \rho(\mathbf{r})[\ln \mathcal{V}\rho(\mathbf{r}) - 1]$$

$$= \ln(\mathcal{V}/\sigma^3) - 1 + 3\int_{-\infty}^{\infty} dx\, g(x)\ln[\sigma s(x)]. \tag{11}$$

The integrand is written in a suitable way to use Gauss–Hermite numerical quadratures.[41] As for the excess contribution, similar manipulations lead to

$$\Psi^{\text{ex}} = \frac{1}{8}\int_{-d/2}^{d/2} dx\, q(x) \int_{-d/2}^{d/2} dy\, q(y)$$

$$\times \int_{-d/2}^{d/2} dz\, q(z)\psi(x,y,z)$$

$$= \frac{1}{8}\int_{-\infty}^{\infty} dx\, g(x) \int_{-\infty}^{\infty} dy\, g(y) \int_{-\infty}^{\infty} dz\, g(z)$$

$$\times \sum_{\{\pm\}} \psi(x \pm \sigma/2, y \pm \sigma/2, z \pm \sigma/2), \tag{12}$$

where the last summation runs over all combinations of signs. Again the latter expression is suitable for Gauss–Hermite integration, which is crucial this time because (12) involves a three-dimensional integration.

We can now minimize with respect to $\alpha$ to determine the equilibrium profile. This yields a continuous freezing at $\eta = 0.348$. As the transition is continuous we can make a more accurate determination of the transition density via a standard bifurcation analysis. This is equivalent to finding the density at which the structure factor diverges for some wavevector $\mathbf{k}_c$. The structure factor is expressed in terms of the direct correlation function (DCF) as $S(\mathbf{k}) = 1/[1 - \rho\hat{c}(\mathbf{k})]$, and the Fourier transform of the DCF, $\hat{c}(\mathbf{k})$, is obtained through Eq. (56) of I for a one-component fluid. In order to simplify the final expression we exploit the symmetry of the crystal by choosing $\mathbf{k}_c = (k_c,0,0)$ (the result would be the same if we chose $k_c$ along the $Y$ or $Z$ axes). Thus the condition to determine the critical point is

$$1 + 2\eta_c \frac{4 - 3\eta_c + \eta_c^2}{(1-\eta_c)^3} j_0(k\sigma) + \eta_c^2 \frac{9 - 4\eta_c + \eta_c^2}{(1-\eta_c)^4} j_0(k\sigma/2)^2$$

$$\geq 0, \tag{13}$$

the equality holding only for $k = k_c$; $j_0(x) \equiv \sin x/x$ is the zeroth order spherical Bessel function. The solution to this equation is $\eta_c = 0.3143\cdots$ and $k_c\sigma = 4.8276\cdots$.

The discrepancy is noticeable between the value of $\eta_c$ obtained from the divergence of the structure factor and that obtained using the profile (1). The reason for this discrepancy can be inferred if we obtain from $k_c$ the lattice spacing, $d_c/\sigma = 2\pi/k_c = 1.3015\cdots$; thus $\eta_c(d_c/\sigma)^3 = 0.6929\cdots$, which means that the resulting crystal has a large fraction of

vacancies (around 31% of the lattice sites!). This is a strong effect that can be accounted for by simply multiplying the r.h.s. of (1a) by an average occupancy ratio $\vartheta$ and minimizing with respect to this new variational parameter. In the calculation process this simply amounts to (i) add a term $\ln \vartheta$ to the ideal free energy (11), and (ii) replace $n_3$ by $\vartheta n_3$ in the definition of $\psi$ [Eq. (10)]. Notice that $d$ is now given by $d = \sigma(\vartheta/\eta)^{1/3}$. As a result we obtain the value of $\eta_c$ given by the bifurcation analysis as well as an occupancy ratio of $\vartheta \approx 0.694$, consistent with the value obtained above[42] (the small discrepancy is due to the Gaussian parametrization we have taken, which is less accurate the larger the mean-square displacement of the particles).

The solid equation of state, with and without vacancies, is plotted in Fig. 1 and compared with the simulations. It is obtained as $\beta P \sigma^3 = \eta^2 \partial \Psi / \partial \eta$. We can see that the overall agreement is good, although the freezing point is shifted down with respect to the simulations because the SPT equation of state overestimates the pressure of the fluid phase.

## III. STABILITY OF THE BINARY FLUID MIXTURE

There are two requirements for a fluid mixture to be stable:[43] (i) the positiveness of the specific heat at constant volume $(c_v)$, and (ii) the positive definiteness of the matrix

$$\mathrm{M}_{ij} \equiv \beta \frac{\partial^2 f}{\partial \rho_i \partial \rho_j} = \frac{1}{\rho_i} \delta_{ij} - \hat{c}_{ij}(\mathbf{0}), \qquad (14)$$

where $f \equiv F/V, F$ being the Helmholtz free energy, $\rho_i$ is the number density of species $i$, and $\hat{c}_{ij}(\mathbf{k})$ is the Fourier transform of the DCF of the mixture [see Eq. (7) of I]. Condition (i) is trivially fulfilled, because any hard core model is athermal, which means that the dependence of the free energy on temperature is that of an ideal gas; hence the positiveness of $c_v$. Condition (ii) is a consequence of the equilibrium state being a minimum of the free energy.

Now, for a binary mixture, M is a $2 \times 2$ matrix with all its elements positive; thus the mixture will be stable provided $|\mathrm{M}| > 0$. The solution to the equation $|\mathrm{M}| = 0$, if it exists at all, will represent a spinodal curve. Such a condition can be understood in terms of the structure factor matrix of the mixture, given by

$$\rho S(\mathbf{k}) \equiv [P^{-1} - \hat{C}(\mathbf{k})]^{-1}, \qquad (15)$$

where $\hat{C}_{ij} \equiv \hat{c}_{ij}$ and $P_{ij} \equiv \rho_i \delta_{ij}$. Then, after (14), $|\mathrm{M}| = 0$ is the condition for the structure factor to diverge at zero wavevector (the uniform fluid).

In order to work out the expression of $|\mathrm{M}|$ let us introduce the following notation: $\eta_i \equiv \sigma_i^D \rho_i$, the packing fraction of species $i$; $\eta \equiv \eta_1 + \eta_2 = \xi_D$, the total packing fraction of the fluid; $r \equiv \sigma_1/\sigma_2$, the large-to-small edge ratio $(r \geq 1)$; and $x \equiv \eta_1/\eta$, the relative packing fraction of the large component. With these definitions as well as the short-hand $\mathcal{M} \equiv \rho_1 \rho_2 |\mathrm{M}|$ we obtain, after a tedious but straightforward calculation,

$$\mathcal{M} = \frac{1 + \eta}{(1 - \eta)^3}, \qquad (16)$$
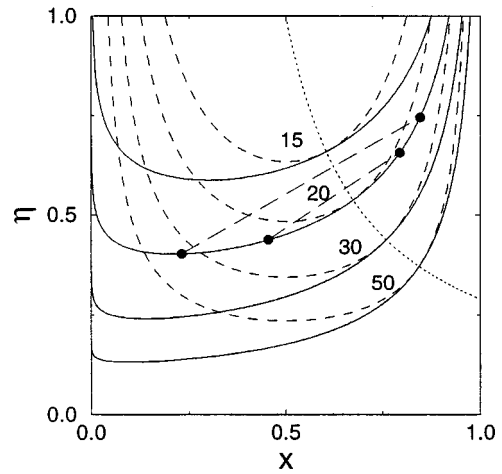
for $D = 2$, and[10]



FIG. 2. Phase diagram of the demixing transition of parallel hard cubes; $\eta$ is the fraction of volume occupied by all cubes, whereas $x \equiv \eta_1/\eta$ is the fraction of volume occupied by the large cubes. Short-dashed lines represent the spinodals for different values of the edge-to-edge ratio; solid lines are the corresponding coexistence lines (the actual transition lines); the dotted line is the line of critical points of the demixing transition for all values of $r > r_c$; finally, the long-dashed segments joining black dots are two examples of coexisting states.

$$\mathcal{M} = \frac{\eta^2}{(1 - \eta)^4} \left[ 1 + \frac{4}{\eta} + \frac{1}{\eta^2} - \frac{3(r-1)^2}{r} x(1-x) \right], \qquad (17)$$

for $D = 3$.

From (16) it follows that the 2D mixture is stable whichever the values of $\eta$, $r$, and $x$. Accordingly, parallel hard squares never demix into two *fluids* with different compositions. Equation (17), however, tells us that the mixture of PHC will be stable provided the expression in square brackets is positive, i.e.,

$$1 + \frac{4}{\eta} + \frac{1}{\eta^2} > \frac{3(r-1)^2}{r} x(1-x). \qquad (18)$$

Since the minimum of the function $1 + 4/\eta + 1/\eta^2$, for $0 \leq \eta \leq 1$, is 6 (reached when $\eta = 1$) and the maximum of $x(1-x)$, for $0 \leq x \leq 1$, is 1/4 (reached when $x = 1/2$), (18) will hold for *any* $\eta$ and $x$ whenever $r^2 - 10r + 1 < 0$, i.e., for any $1 < r < r_c = 5 + \sqrt{24} \approx 9.98$. For $r \geq r_c$ there will exist values of $\eta$ and $x$ for which (18) does not hold, and thus the mixture demixes. From (18) it is very simple to find that those values correspond to the region above the curve

$$\frac{1}{\eta} = \sqrt{3} \sqrt{1 + \frac{(r-1)^2}{r} x(1-x)} - 2, \qquad (19)$$

which therefore defines the spinodal. Figure 2 shows this curve for a few values of $r$. It is interesting to notice the symmetry of the spinodal with respect to $x = 1/2$. This means that for a given packing fraction, $\eta$, the stability of the mixture depends on the fraction of occupied volume of any of the particles, regardless their type, large or small.

The existence of a spinodal instability of this type means that if the system is kept at constant pressure, there is a certain region in the density-composition phase diagram in which the fluid is stable in two coexisting phases, one rich in small particles and the other one rich in large particles. In

order to determine the values of $\eta$ and $x$ of the two coexisting phases we must solve the equilibrium equations $P(\eta_s,x_s)=P(\eta_l,x_l)=p$,  $\mu_i(\eta_s,x_s)=\mu_i(\eta_l,x_l)$,  $i=1,2$, where the subindex $s(l)$ labels the small-particle (large-particle) rich phase, and $p$ is the externally fixed pressure. The critical point of this transition for a given ratio $r$ is determined as the point of the spinodal (19) where the pressure reaches a minimum.

The phase diagram (Fig. 2) shows a few features that are worth noticing. First of all, it is interesting to see that the critical line collides, when $r\to\infty$, with the $x=1$ edge of the phase diagram at a nonzero packing fraction. What this suggests is that in this limit the packing fraction of the small component goes to zero but it still remains a residual depletion between the large cubes. This depletion forces the one-component effective fluid of large cubes to collapse beyond a certain packing fraction. We will explore this matter in full detail in Sec. V.

Another interesting feature of the phase diagram is the remaining impurity of the two separated phases even when the system undergoes an infinite pressure. This reflects the fact that the coexistence lines end up at values of $x$ other than 1 or 0 (pure components) when $\eta=1$ (actually, this effect is noticeable only for the values of the large-cube rich phase, although it is also present in the other phase). The prominent asymmetry of the coexistence line is another striking feature, but easy to understand: it arises from the enormous volume difference between large and small cubes necessary to produce demixing (notice that demixing begins for $r\approx10$, and this means that large cubes occupy a volume 1000 times larger than the small ones). This forces the large-cube impurities in the small-cube rich phase to be in an extremely low concentration. The wide metastability region in the small-cube rich side means that for those compositions the mixture is less sensitive to variations in composition.

## IV. FREEZING OF THE BINARY MIXTURE

In order to check to which extent the demixing scenario found in the previous section holds, we have to determine whether the fluids are stable against spatial modulations at the coexisting compositions. Spatial inhomogeneities cause a divergence of the structure factor matrix (15) at a certain nonzero wavevector. Thus for a given composition, $x$, the spatial instability is found as the lowest total packing fraction at which the determinant $\mathcal{M}(\mathbf{k})\equiv|P^{-1}-\hat{C}(\mathbf{k})|$ vanishes for at least one vector $\mathbf{k}$. We can use the expression for the DCF found in I [Eqs. (53), (54), and (57) of I] and simplify the problem by simply looking for instabilities along the three coordinate axes. By symmetry, this amounts to taking $\mathbf{k}=(k,0,0)$.

The value of $\eta$ at which $\mathcal{M}(\mathbf{k})=0$, as a function of $x$, is plotted in Fig. 3 for different values of $r$; these lines of instability are compared with the coexistence lines of the demixing transition (Fig. 2). It is clear from the figure that the critical points of the latter are always in the unstable region; therefore, for any pair of coexisting fluids, at least one (the large-cube rich one) is always unstable against spatial inhomogeneities. In other words, of the two phases in which the
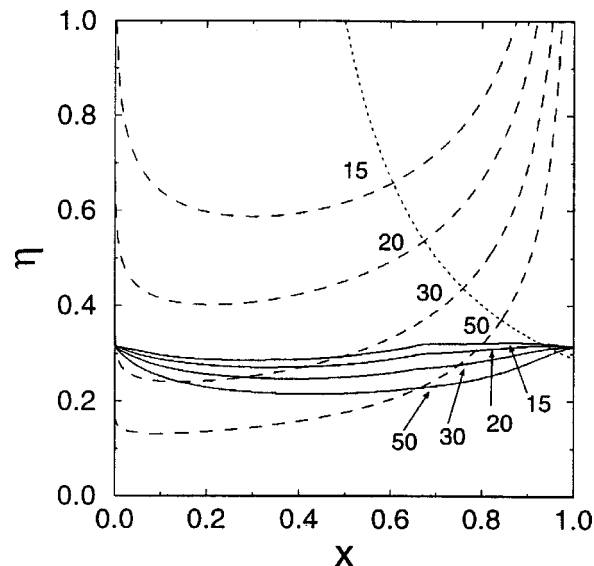


FIG. 3. Phase diagram of the demixing transition of parallel hard cubes; $\eta$ is the fraction of volume occupied by all cubes, whereas $x\equiv\eta_1/\eta$ is the fraction of volume occupied by the large cubes. Dashed lines represent the coexistence lines of the demixing transition for different values of $r=\sigma_1/\sigma_2$; solid lines are the freezing spinodals for the same values of $r$; finally, the dotted line is the line of critical points for all $r>r_c$.

system phase separates, the one rich in large cubes must always be a solid. Notice, on the other hand, that the other phase is also unstable for size ratios smaller than $r\approx30$. One is then tempted to conclude that fluid–fluid demixing is pre-empted by freezing in this system. However coexistence between a large-cube rich solid phase and a small-cube rich fluid phase may change drastically the compositions of the coexisting phases and thus make a fluid–solid demixing more stable than just a freezing of the whole system. The only conclusion we can draw from Fig. 3 is that the fluid–fluid demixing transition found in Sec. III is always metastable.

## V. INFINITELY ASYMMETRIC BINARY MIXTURE: PARALLEL ADHESIVE HARD CUBES

### A. The binary mixture as an effective one-component fluid

In order to study the phase behavior of a very asymmetric binary mixture let us first consider the effect on the interaction of the big particles induced by the small ones (depletion). To this purpose let us use a semigrand ensemble in which the small particles (solvent) are kept at constant chemical potential. In this situation the element of the structure–factor matrix (15) corresponding to the correlations between large particles can be considered as the structure factor of an equivalent one-component fluid made of the large particles interacting via the effective potential induced by the solvent. This turns out to be a very useful viewpoint. Let us see how this comes about.

The appropriate thermodynamic potential for the semigrand ensemble is obtained through a Legendre transformation of the Helmholtz free energy, namely

$$\Upsilon(\mu_2,[\rho_1]) = F[\rho_1,\rho_2] - \mu_2 \int \rho_2, \qquad (20)$$

$$\mu_2 = \frac{\delta F}{\delta \rho_2(\mathbf{r})} = \beta^{-1} \ln \mathcal{V}_2 \rho_2(\mathbf{r}) + \frac{\delta F^{\mathrm{ex}}}{\delta \rho_2(\mathbf{r})}, \qquad (21)$$

where Eq. (21) provides the equilibrium density of the solvent for a given chemical potential $\mu_2$ and a solute density profile $\rho_1(\mathbf{r})$, thus allowing us to eliminate $\rho_2(\mathbf{r})$ from the r.h.s. of (20). The thermodynamic potential $\Upsilon$ can also be looked at as the *Helmholtz free energy* functional of an effective one-component fluid, for which $\mu_2$ is just an external parameter tuning the interaction between its particles. Accordingly we can separate out the ideal and excess parts,

$$\Upsilon = \beta^{-1} \int \rho_1 [\ln(\mathcal{V}_1 \rho_1) - 1] + \Upsilon^{\mathrm{ex}}, \qquad (22)$$

where, upon comparison with (20),

$$\Upsilon^{\mathrm{ex}} \equiv \beta^{-1} \int \rho_2 [\ln(\mathcal{V}_2 \rho_2) - 1] + F^{\mathrm{ex}} - \mu_2 \int \rho_2, \qquad (23)$$

with $\rho_2$ determined by Eq. (21).

Now, the DCF of the effective fluid will be

$$c_{\mathrm{eff}}(\mathbf{r},\mathbf{r}') = -\beta \frac{\delta^2 \Upsilon^{\mathrm{ex}}}{\delta \rho_1(\mathbf{r}) \delta \rho_1(\mathbf{r}')}. \qquad (24)$$

Then, from (24), the usual DCF matrix definition $c_{ij}(\mathbf{r},\mathbf{s}) = -\beta \delta^2 F^{\mathrm{ex}} / \delta \rho_i(\mathbf{r}) \delta \rho_j(\mathbf{s})$, and introducing the shorthand $A(\mathbf{r},\mathbf{s}) \equiv \delta \rho_2(\mathbf{s}) / \delta \rho_1(\mathbf{r})$, the effective DCF can be expressed as

$$c_{\mathrm{eff}}(\mathbf{r},\mathbf{r}') = c_{11}(\mathbf{r},\mathbf{r}') + \int d\mathbf{s}\, A(\mathbf{r},\mathbf{s}) c_{21}(\mathbf{s},\mathbf{r}'). \qquad (25)$$

The functional $A(\mathbf{r},\mathbf{s})$ can be readily obtained by deriving (21) with respect to $\rho_1(\mathbf{r})$, which leads to

$$\int d\mathbf{t} \left\{ \frac{1}{\rho_2(\mathbf{r})} \delta(\mathbf{r}-\mathbf{t}) - c_{22}(\mathbf{r},\mathbf{t}) \right\} A(\mathbf{t},\mathbf{s}) = c_{12}(\mathbf{r},\mathbf{s}). \qquad (26)$$

These expressions have full generality: they are valid for any binary mixture of any kind and in any particular phase. But we can get a bit further if we particularize for the uniform fluid. In this case the density profiles are constant and all the above functions depend on the difference of their arguments, because of translational invariance. Then, Fourier transforming Eqs. (25) and (26) we can elliminate $A$ and write

$$\hat{c}_{\mathrm{eff}}(\mathbf{k}) = \hat{c}_{11}(\mathbf{k}) + \frac{\rho_2 \hat{c}_{12}(\mathbf{k})^2}{1 - \rho_2 \hat{c}_{22}(\mathbf{k})}. \qquad (27)$$

In order to understand the meaning of Eq. (27) let us compute the structure factor of the effective fluid:

$$\rho_1 S_{\mathrm{eff}}(\mathbf{k}) = \frac{1}{\rho_1^{-1} - \hat{c}_{\mathrm{eff}}(\mathbf{k})} = \frac{\rho_2^{-1} - \hat{c}_{22}(\mathbf{k})}{|P^{-1} - \hat{C}(\mathbf{k})|}; \qquad (28)$$

the resulting expression is but the (1,1)-element of the structure-factor matrix $\rho \hat{S}(\mathbf{k})$, according to its definition (15). This was, by the way, the starting point from which the effective fluid was defined in Ref. 38.
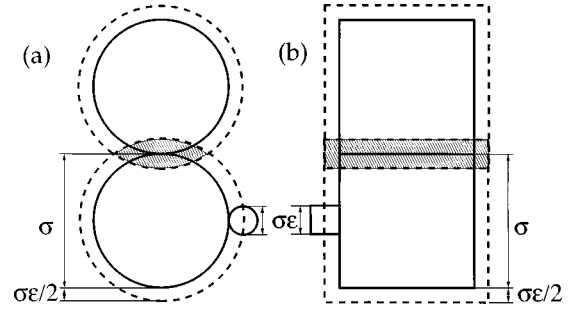


FIG. 4. Increment in the total volume, $\Delta V$, available to the small particles when two large particles come to touch each other (shaded region). If $v_0$ denotes the volume of a large particle, $\Delta v$ is (a) $v_0 \epsilon^2 (3/2 + \epsilon)$ for HS, and (b) $v_0 \epsilon (1 + \epsilon)^2$, for PHC.

Further insight can be gained if we expand (27):

$$\hat{c}_{\mathrm{eff}}(\mathbf{k}) = \hat{c}_{11}(\mathbf{k}) + \rho_2 \sum_{n=0}^{\infty} \rho_2^n \hat{c}_{12}(\mathbf{k}) [\hat{c}_{22}(\mathbf{k})]^n \hat{c}_{21}(\mathbf{k}), \qquad (29)$$

where it can be explicitly seen that while the first term in (27) represents the direct correlation between two solute particles via the direct potential between them, the second term accounts for the indirect contributions to this correlation due to interaction with one, two, three, etc., intermediate solvent particles. This is the effect that accounts for depletion in the binary mixture of hard particles.

## B. Depletion in the binary mixture of parallel hard cubes

Let us first compare the effective attraction between large particles induced by the small ones (depletion). A simple way to achieve this is by computing the work we have to make against the system in order to separate two big particles further than the diameter of a small one. This work will be simply $P\Delta V$, with $P$ the pressure of the fluid and $\Delta V$ the free volume lost by the small particles due to the disappearance of the overlap between the excluded regions of the large particles (shaded in Fig. 4).

In the case of HS, $\Delta V = (3v_0/2)\epsilon^2 + O(\epsilon^3)$, with $v_0$ the volume of a big sphere and $\epsilon$ the small-to-large diameter ratio. It means that in the diluted regime of the small particles $(P \sim \rho_2)$ this work can be estimated as $\sim \beta^{-1}(3/2)\eta_2/\epsilon$. In the case of PHC, $\Delta V = v_0\epsilon + O(\epsilon^2)$, with $v_0$ the volume of a big cube and $\epsilon$ the small-to-large edge–length ratio. Again in the diluted regime of the small cubes the work is $\sim \beta^{-1}\eta_2/\epsilon^2$. In other words, the depletion induced by PHC is much stronger than that induced by HS. In the infinite asymmetry limit, the binary mixture HS has been shown to reduce to the fluid of adhesive HS, provided $\eta_2$ is kept constant.[38] According to our estimation, in order to have a similar limit for the binary mixture of PHC we must scale the packing fraction of the small cubes as $\eta_2 = \epsilon\xi$, with $\xi$ a constant.

We can now assume this scaling of $\eta_2$ and take the $\epsilon \to 0$ limit in Eq. (27). A tedious but straightforward calculation leads to

$$c_{\mathrm{eff}}(\mathbf{r}) = c_{\mathrm{PHC}}(\mathbf{r}) + c_{\mathrm{ad}}(\mathbf{r}), \qquad (30)$$

$$c_{\mathrm{ad}}(\mathbf{r}) = \frac{\xi}{2(1-\eta)^2}\{\delta_S(\mathbf{r}) + yS(\mathbf{r}) + 6y^2 V(\mathbf{r})\}, \qquad (31)$$

where $y \equiv \eta_1/(1-\eta_1)$, $c_{\mathrm{PHC}}(\mathbf{r})$ is the DCF of the one-component PHC fluid [Eq. (56) of 1], and

$$\delta_S(\mathbf{r}) = A(x,y,z) + A(y,z,x) + A(z,x,y), \qquad (32)$$

$$A(u,v,w) \equiv \delta(\sigma_1 - |u|)L(v)L(w), \qquad (33)$$

$$L(u) \equiv (\sigma_1 - |u|)\Theta(\sigma_1 - |u|). \qquad (34)$$

Equation (32) represents a delta function at contact of two large cubes, multiplied by the contact surface. The functions $S(\mathbf{r})$ and $V(\mathbf{r})$ are the overlap surface and volume, respectively, which already appear in the definition of $c_{\mathrm{PHC}}$ [Eq. (53) of 1]. In the zero density limit $c_{\mathrm{eff}}(\mathbf{r}) \sim f(\mathbf{r}) + \xi \delta_s(\mathbf{r})$, with $f(\mathbf{r})$ the Mayer function of the large cubes; so, as in HS, in the infinitely asymmetric mixture depletion induces an adhesive potential (in this case, of strength $\xi$).

Notice that in both cases (HS[38] and PHC) the $\epsilon \to 0$ limit has been taken such that the structure factor of the resulting effective fluid differs from that of the one-component fluid in a finite nonzero correction. To define the adhesive HS model Baxter made the same assumption with respect to the second virial coefficient (in this case the limit is that of an infinitely deep and narrow square well). Both assumptions are equivalent. For this reason we will henceforth refer to our effective fluid as the fluid of *parallel adhesive hard cubes* (PAHC).

## C. Free-energy functional of the fluid of parallel adhesive hard cubes

Let us now take the $\epsilon \to 0$ limit in the functional (20) to obtain the Helmholtz free-energy functional for the fluid of PAHC. In the limit we will find that $\Upsilon \to \infty$; however, this is not a problem as long as for *every* fixed $\epsilon$ there is a well-defined functional giving rise to a phase behavior which does have a finite limit when $\epsilon \to 0$. We will show that this is the case, and thus this functional will be the effective functional we are looking for. We will see that the infinite contribution is just a *constant* shift in the origin of free energies, absolutely irrelevant for the phase behavior.

Let us begin by recalling what FMT prescribes for the semigrand potential (20). It is convenient to introduce two dimensionless densities, $\eta(\mathbf{r}) \equiv \sigma_1^3 \rho_1(\mathbf{r})$, and $\xi(\mathbf{r}) \equiv \sigma_1^3 \epsilon^2 \rho_2(\mathbf{r})$. [There is no possible confusion between the function $\eta(\mathbf{r})$ and the total packing fraction, because when $\epsilon \to 0$ the total packing fraction is simply the packing fraction of the large component, i.e., the average of $\eta(\mathbf{r})$.] In what follows we will fix the unit length of our system by choosing $\sigma_1 = 1$. In terms of these functions the FMT form of the functional (20) is

$$\beta \Upsilon = \beta \bar{F}^{\mathrm{id}} + \int d\mathbf{r}\, \Phi(\mathbf{r})$$

$$+ \epsilon^{-2} \int d\mathbf{r}\, \xi(\mathbf{r})(\ln[\xi(\mathbf{r})/z] - 1), \qquad (35)$$

$$\beta \bar{F}^{\mathrm{id}} = \int d\mathbf{r}\, \eta(\mathbf{r})(\ln[\mathcal{V}_1 \eta(\mathbf{r})] - 1), \qquad (36)$$

where we have defined the renormalized fugacity $z \equiv \epsilon^2 \exp(\beta \mu_2^{\mathrm{ex}})$, $\mu_2^{\mathrm{ex}} \equiv \mu_2 - \beta^{-1} \ln V_2$. Equation (36) is just the ideal Helmholtz free energy of the effective fluid, and $\Phi(\mathbf{r})$ is given by (5), where, in the current notation, $n_\alpha = \eta * \omega_1^{(\alpha)} + \epsilon^{-2}\xi * \omega_2^{(\alpha)}$. But $\xi(\mathbf{r})$ is a dependent variable which should be eliminated in terms of $\eta(\mathbf{r})$ and $\mu_2$ via Eq. (21), which in our case reads

$$\ln \xi(\mathbf{r}) = \ln z - \sum_\alpha \frac{\partial \Phi}{\partial n_\alpha} * \omega^{(\alpha)}(\mathbf{r}). \qquad (37)$$

For $\xi(\mathbf{r})$ to have a well-defined expansion in powers of $\epsilon$,

$$\xi = \xi_0 + \xi_1 \epsilon + \xi_2 \epsilon^2 + O(\epsilon^2), \qquad (38)$$

we are forced to assume $z = O(1)$. Then we can expand (37) and determine the functions $\xi_i$ in terms of $\eta$ and $z$ (the actual expression for $\xi_2$ turns out to be unnecessary in the final expressions). By further expanding Eq. (35) we finally obtain

$$\Upsilon = -\Pi_0(\epsilon)V + \mu_0(\epsilon)N + \bar{F} + F^{\mathrm{ad}} + O(\epsilon) \qquad (39)$$

(the details appear in the Appendix). In this equation $\bar{F}$ is the FMT free-energy functional of the fluid of the large PHC; $V$ and $N$ are, respectively, the system volume and the number of large cubes; $F^{\mathrm{ad}} = \int \Phi^{\mathrm{ad}}$, with

$$\Phi^{\mathrm{ad}} \equiv \frac{z}{8} \frac{|\nabla \bar{n}_3|^2 - 4\bar{\mathbf{n}}_2 \cdot \bar{\mathbf{n}}_2}{1 - \bar{n}_3}, \qquad (40)$$

is the new adhesive term; and $\Pi_0$ and $\mu_0$ are functions of $z$ and $\epsilon$, but not of $\eta$.

The term $-\Pi_0(\epsilon)V + \mu_0(\epsilon)N$ diverges with $\epsilon \to 0$ as $O(\epsilon^{-2})$. It is the contribution of the small cubes to the free energy (as a matter of fact, their density is infinite in this limit). However it is irrelevant for the phase behavior of the effective fluid because it simply adds $\Pi_0$ to the pressure and $\mu_0$ to the chemical potential; as these two terms are independent of the density, they just cancel out in the equilibrium equations. Accordingly the final free-energy functional for the effective one-component PAHC fluid turns out to be

$$F_{\mathrm{PAHC}}([\rho];z) = F_{\mathrm{PHC}}[\rho] + F^{\mathrm{ad}}([\rho];z). \qquad (41)$$

As a selfconsistency test, it is straightforward to show [using Eq. (A1)] that $c^{\mathrm{ad}}(\mathbf{r} - \mathbf{r}') = -\beta \delta^2 F^{\mathrm{ad}}/\delta\rho(\mathbf{r})\delta\rho(\mathbf{r}')$, for the $c^{\mathrm{ad}}$ function defined in (31).

## D. Phase behavior of the infinitely asymmetric binary mixture

The phase behavior of a very asymmetric binary mixture of PHC can be understood from that of the effective fluid of PAHC whose FMT free-energy functional we have just derived.

As concerns the phase behavior of the uniform PAHC fluid, from (41), (5), and (40) we can readily obtain the free energy per unit volume,

$$\beta f = \eta\{\ln \mathcal{V}_1 - 1 + \ln y + 3(1 - z/2)y + y^2\}. \qquad (42)$$

The pressure, $P = -\partial F/\partial V = y^2 \partial(f/\eta)/\partial y$, turns out to be
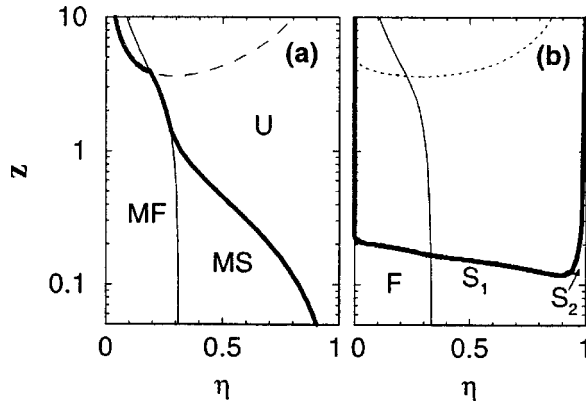
$$\beta P = y + 3(1 - z/2)y^2 + 2y^3. \qquad (43)$$

FIG. 5. Solvent fugacity, $z$, vs solute packing fraction, $\eta$, of the infinitely asymmetric binary mixture of PHC, both without (a) and with (b) polydispersity ($\Delta\sigma/\sigma = 4.5\%$). (a) The thick solid line separates the unstable region (U) from the metastable one; the thin one marks the (continuous) transition from a metastable fluid (MF) to a metastable solid (MS); the dashed one is the fluid–fluid spinodal. (b) The thick solid line marks the fluid–solid or solid–solid coexistence; the thin one marks again the (continuous) fluid–solid transition below the coexistence region; the dotted line is the metastable fluid–fluid coexistence.

This equation has a van der Waals loop with a critical point ($\partial P/\partial\eta = 0$, $\partial^2 P/\partial\eta^2 = 0$) at $z_c = 2(1+\sqrt{2/3}) \approx 3.63$ and $\eta_c = 1/(1+\sqrt{6}) \approx 0.29$. On the other hand, the equation of the spinodal ($\partial P/\partial\eta = 0$) of this vapor–liquid transition is

$$z = \frac{1+4\eta+\eta^2}{3\eta(1-\eta)}; \tag{44}$$

it is plotted in Fig. 5(a). Notice that this spinodal could have been obtained directly from (17) by taking the limit $r\to\infty$, $x\to 1$, under the constraint $r\eta(1-x) = \xi \to z(1-\eta)$ [the limit follows from (A1)]. Thus it is not surprising that the line of critical points in Fig. 2 reaches $\eta_c$ for $x\to 1$. This makes clear the double interpretation of this transition: as a vapor–liquid transition of the PAHC fluid (with $z^{-1}$ playing the role of a temperature), or as a demixing transition of the infinitely asymmetric binary mixture.

Freezing of this system into a simple cubic lattice is again a continuous transition. Hence the transition line can be determined by the procedure described in Sec. II, i.e., as the divergence of the structure factor, now given by the effective DCF (30). The result is the line shown in Fig. 5(a). As it occurred for the general binary mixture (see Sec. III), the freezing line crosses the demixing spinodal at a packing fraction smaller than $\eta_c$; in other words fluid–fluid demixing is a metastable transition.

So far we have gone no further than we did in Secs. III, IV. However this time we can study fluid–solid coexistence because the density profile of the solvent is absent from the description. To proceed we again parametrize the density of the large cubes as in (1), also with a prefactor $\vartheta$ to account for vacancies. We recall that the lattice parameter is related to this occupancy ratio by $d = (\vartheta/\eta)^{1/3}$. The ideal contribution to the free energy per particle, $\Psi$, is again given by (11) (adding $\ln\vartheta$ from the vacancies), and the hard-core part of the excess contribution is given by (12) [with $n_3(\mathbf{r}) = \vartheta p(x)p(y)p(z)$]. We now need to work out the adhesive term. To this purpose first notice that

$$p'(u)^2 - q(u)^2 = -4s(u+1/2)s(u-1/2); \tag{45}$$

hence the adhesive free energy per particle can be written

$$\Psi^{\mathrm{ad}} = -\frac{3}{2}\vartheta z\int_{-\infty}^{\infty} dx\, g(x)s(x+1)U(x+1/2), \tag{46}$$

where $U(x)$ is defined as

$$U(x) \equiv \int_{-d/2}^{d/2} dy \int_{-d/2}^{d/2} dz\, \frac{p(y)^2 p(z)^2}{1-\vartheta p(x)p(y)p(z)}, \tag{47}$$

and it is periodic with period $d$ [we have made use of periodicity in obtaining (46)].

It is convenient to rewrite Eq. (47) integrating by part with respect to both variables, $y$ and $z$; in doing so this equation becomes

$$U(x) = \int_{-d/2}^{d/2} dy\, p'(y) \int_{-d/2}^{d/2} dz\, p'(z) V(x,y,z), \tag{48}$$

$$V(\mathbf{r}) \equiv T(y)p(y)T(z)p(z) \frac{4-3n_3(\mathbf{r})+3n_3(\mathbf{r})^2}{1-n_3(\mathbf{r})}, \tag{49}$$

where $T(u) = u$ if $u \in (-d/2, d/2)$ [the only relevant interval in (48)] and it is $d$-periodic. Function $V(x,y,z)$ is then also $d$-periodic in all its three arguments; accordingly Eq. (48) can be rewritten as

$$U(x) = \int_{-\infty}^{\infty} dy\, g(y) \int_{-\infty}^{\infty} dz\, g(z) W(x,y,z), \tag{50}$$

$$W(x,y,z) \equiv \sum_{\tau_1,\tau_2 = \pm 1} \tau_1\tau_2 V(x,y+\tau_1/2, z+\tau_2/2), \tag{51}$$

and therefore

$$\Psi^{\mathrm{ad}} = -\frac{3}{2}\vartheta z\int_{-\infty}^{\infty} dx\, g(x) \int_{-\infty}^{\infty} dy\, g(y) \int_{-\infty}^{\infty} dz\, g(z)$$
$$\times s(x+1)W(x+1/2,y,z), \tag{52}$$

also suitable for Gauss–Hermite numerical integration.

In order to understand the effect of the adhesive contribution (46) let us see its asymptotic behavior when $\alpha\to\infty$ and $d\to 1^+$ (equivalently $\vartheta\to\eta^+$), a limit which would represent a close-packed solid. From its definition (7) $p(u)\sim 1$ in this limit; thus $U(x)\sim 1/(1-\eta)$. On the other hand, $g(u)$ is very sharply peaked, so

$$\int_{-\infty}^{\infty} dx\, g(x)s(x+1) \sim g(0) = \left(\frac{\alpha}{\pi}\right)^{1/2},$$

therefore $\Psi^{\mathrm{ad}} \sim -(3/2)z(\alpha/\pi)^{1/2}/(1-\eta)$. On the other hand $\Psi^{\mathrm{ex}} = O(1)$ in this limit, while $\Psi^{\mathrm{id}} \sim 3\ln g(0) \sim (3/2)\ln\alpha$. In other words, the total free energy per particle of the effective fluid monotonically decreases as the system approaches the close packing, regardless the value of density and solvent fugacity. This means that the system always collapses, i.e., the equilibrium phase behavior is always a close-packed solid coexisting with an infinitely diluted gas. This singular phase diagram is not exclusive of PAHC. For adhesive HS, the adhesiveness vs. packing fraction phase diagram ($z$ plays the role of adhesiveness for PAHC) has recently been mapped out from simulations of the square-well fluid in the

limit of narrow and deep wells.[34] These simulations prove that the only stable phases of this system are also a close-packed solid and an infinitely diluted gas. The reason for this pathology was put forward some years ago by Stell,[44] who showed that the partition function of the adhesive HS model diverges if the number of particles is $N \geq 12$. In his work Stell discusses a new limit in which the adhesiveness goes to zero (hence the second virial coefficient reduces to that of HS) in such a way that there appears a critical temperature separating the singular phase behavior (below) from a HS-like phase behavior (above). It is not clear how this limit can be implemented in our formalism without completely suppressing depletion, so in what follows we will just limit ourselves to the analog of Baxter's model we have defined and will try to extract some consequences.

In spite of the singular phase behavior we have seen that, as a function of $\alpha$ and $\vartheta$, the free energy per particle exhibits local minima at any value of $z$ for some range of densities, the smaller $z$ the wider this range. These local minima correspond to metastable phases. Although we cannot rule out that the existence of these states is but an artifact of the particular parametrization we have chosen, they are likely to exist in view of the very long times clusters of large particles take to evolve in simulations.[31] The upper bound to the packing fractions at which local minima exist for a given $z$ can be determined as the point where the compressibility vanishes. This upper bound, as a function of $z$, appears in Fig. 5(a). This figure shows the metastable phases. Notice that the region of metastability widens as $z$ decreases. At low $z$ these metastable phases are separated from the ''collapse'' by a large free-energy barrier, so the system spends a long time in them before eventually becoming a close-packed solid. As a matter of fact, if the system is prepared as a metastable solid at low $z$, for a long time it will show a pseudocoexistence between two solid phases (an expanded solid and a close-packed solid). The situation resembles the isostructural solid–solid transition reported to occur in some colloidal fluids with a narrow and deep attractive well.[34,35] At higher $z$ the same pseudocoexistence should be observed between a diluted fluid and a close-packed solid.

It is interesting to compare this phase behavior with what has been determined to occur for adhesive HS using an effective-liquid DFT.[45] Fluid and solid also appear as local minima of the free energy per particle as a function of the Gaussian width; however, above a certain line the free energy becomes concave up to close packing. This puzzling behavior was interpreted in Ref. 45 as a percolation transition. In the light of our findings it is the equivalent to the instability line of Fig. 5(a). The fluid of adhesive HS also collapses into a close-packed solid.[34] The reason why this collapse has not been observed in Ref. 45 is that the theory used there does not account for vacancies, and this forces the lattice parameter to be larger than 1 at *any* packing fraction. The instability manifests itself as the reported loss of convexity of the free energy.

### E. Polydispersity in the large cubes

It has been suggested that the singularity of the adhesive potential might be avoided by introducing polydispersity in the size of the particles.[44,46] It is clear that this prevents the system from forming a perfectly packed solid. We can speculate what its effect is on the binary mixture by introducing a small amount of polydispersity in the size of the large cubes. It is very easy to realize that starting off from a mixture of polydisperse large cubes and small cubes and repeating the process described in Sec. V C we end up with exactly the same form of the functional (41), with the $\bar{n}_\alpha$'s now replaced by those corresponding to the polydisperse mixture.

In order to make the simplest choice we consider the cubes as parallelepipeds and choose the length of each axis independently from a Gaussian distribution of mean 1 and variance $\Delta\sigma$. This particular choice has two important advantages (they will be made clear below): (i) the free energy of the fluid phase is the same as that of the monodisperse system (hence its phase behavior as well), and (ii) formally the expressions for the free energy of the solid phase change very little. It also has two drawbacks: (i) particles are not cubic anymore, and (ii) there is a nonzero contribution in the negative lengths. As these two inconvenients disappear when $\Delta\sigma \to 0$ they can be overcome by choosing $\Delta\sigma \ll 1$. This choice also allows us to make two more simplifying assumptions: (i) the ordered phase must be a substitutional solid, i.e., the density profile can be expressed as $\rho(\mathbf{r})\mathcal{P}(\boldsymbol{\sigma})$, with $\mathcal{P}$ the normalized size distribution, $\boldsymbol{\sigma} \equiv (\sigma_x, \sigma_y, \sigma_z)$, and (ii) phase separation induced by polydispersity[47] can be ignored.

Then, according to the definition of the $\bar{n}_\alpha$'s

$$\bar{n}_\alpha(\mathbf{r}) = \int d\boldsymbol{\sigma}\, \mathcal{P}(\boldsymbol{\sigma}) \rho * \omega_{\boldsymbol{\sigma}}^{(\alpha)}(\mathbf{r}) = \rho * \tilde{\omega}^{(\alpha)}(\mathbf{r}), \tag{53}$$

i.e., it has the same definition as in the monodisperse case, but the weights are redefined as $\tilde{\omega}^{(\alpha)}(\mathbf{r}) \equiv \int d\boldsymbol{\sigma}\, \mathcal{P}(\boldsymbol{\sigma}) \omega_{\boldsymbol{\sigma}}^{(\alpha)}(\mathbf{r})$. This amounts to replacing $\theta^u$ and $\delta^u$ in (4) by

$$\tilde{\theta}^u = \frac{1}{2}\left[1 - \mathrm{erf}\left(\sqrt{2}\,\frac{|u| - 1/2}{\Delta\sigma}\right)\right], \tag{54a}$$

$$\tilde{\delta}^u = \frac{1}{\sqrt{2\pi}\Delta\sigma} \sum_{\{\pm\}} \exp\left\{-2\,\frac{(u \pm 1/2)^2}{\Delta\sigma^2}\right\}, \tag{54b}$$

which are like smoothed counterparts of the original weights. Since $\int_{-\infty}^{\infty} du\, \tilde{\theta}^u = \int_{-\infty}^{\infty} du\, \tilde{\delta}^u = 1$, it follows that the free energy of the uniform fluid is the same as that of the monodisperse system. Hence the fluid–fluid spinodal is the same as that shown in Fig. 5(a).

We can determine the coexistence between the two fluid phases by means of the usual double tangent construction.[43] Figure 5(b) shows the resulting coexistence line.

We can also assume a solid-like density profile as in the monodisperse case. Surprisingly enough, in spite of the striking difference of the smoothed weights defined by (54) with respect to the original ones, when we obtain the corresponding weighted densities and work out the expressions a little bit, it turns out that the free energy per particle of the polydisperse solid is simply given by $\Psi = \Psi^{\mathrm{poly}} + \Psi^{\mathrm{id}} + \Psi^{\mathrm{ex}} + \Psi^{\mathrm{ad}}$, where the last three contributions are given by Eqs. (11), (12), and (52), with the slight modification that the parameter $\alpha$ appearing in the definitions (1c) and (6) must be replaced by $\tilde{\alpha} = \alpha/(1 + \alpha\Delta\sigma^2/2)$ (of course, in these expres-

sions $\sigma = 1$, the mean value, and $\Psi^{id}$ carries the additional $\ln \vartheta$ to account for vacancies), and where $\Psi^{poly} = -3\ln(\sqrt{2\pi}\Delta\sigma) - 3\sqrt{\pi/2}\Delta\sigma$ is the entropy of mixing (an irrelevant constant).

From the definition of $\tilde{\alpha}$ it can be seen that no matter how small $\Delta\sigma$ be, for small $\alpha$'s ($\alpha \ll \Delta\sigma^{-2}$) $\tilde{\alpha} \sim \alpha$, and the system is "blind" to polydispersity, whereas for large $\alpha$'s ($\alpha \gg \Delta\sigma^{-2}$) $\tilde{\alpha} \sim 2\Delta\sigma^{-2}$, i.e., the system never collapses. As a consequence the singular behavior of the monodisperse system is removed, and we can readily determine phase equilibria.

Clearly this behavior is a consequence of the metastable phase diagram discussed in the previous section, and, as in that case, it can be argued to be an artifact of the approximations of the theory. Again we believe the stabilization by polydispersity to be a real effect because it precludes singular clusters to form. Anyway a confirmation by computer simulations would be desirable to clarify this point.

A typical result for a small value of $\Delta\sigma$ is shown in Fig. 5(b). This figure reveals several remarkable features. Firstly, it shows that the fluid–fluid transition is metastable. Secondly, there is an isostructural solid–solid transition for a certain interval of $z$. In this interval the expanded solid ($S_1$) appears after a continuous transition from the fluid phase ($F$). The expanded solid ($S_1$)–dense solid ($S_2$) transition ends at a critical point, $z_s$, below which we can only find a fluid and a single solid, separated by a continuous transition. Thirdly, as $z$ increases from $z_s$ the expanded solid packing fraction decreases down to meeting the freezing packing fraction. Above the point where this occurs coexistence is between a fluid and a dense solid ($S_2$), the former quickly becoming highly diluted and the latter highly packed. Notice the strong resemblance between this true equilibrium phase behavior and the metastable behavior described as occurring in the monodisperse PAHC fluid (Sec. V D).

## VI. DISCUSSION AND CONCLUSIONS

The fluid of PHC is a rather academic one which however has the great advantage of being analytically tractable in contexts where the fluid of HS is not, thanks to its adequacy to a fundamental measure description. Yet, with some peculiarities due to the lack of rotational symmetry,[8,7] the physics it reveals is similar to that of more realistic fluids. It then allows for theoretical investigation on fluid phase behavior otherwise very difficult. The main contribution of the fluid of PHC is to the understanding of the phase diagram of a binary mixture. This fluid proved to undergo stronger depletion than HS.[9,10] However, as it has been shown in this work, this feature is irrelevant when the effect of depletion in the solid phase is accounted for. Spatial order of the large component strongly enhances demixing, so that fluid–solid demixing becomes the main scenario of the phase diagram of binary mixtures. But this transition can be preempted by the freezing of the large component, and when this happens the system phase separates into two fcc solids with a different lattice parameter. This effect, very clearly shown here for the mixture of PHC (in the limit of infinite asymmetry), has also been confirmed in simulations of HS interacting via an ef-

fective depletion potential,[32,33] and very recently also in direct simulations on the true binary mixture.[36] The simulations also show that the solid–solid transition disappears as the asymmetry of the two components decreases, but it is anyhow categoric with respect to the fluid–solid nature of demixing.

A final remark concerns the two-dimensional mixture. We have made preliminary calculations in this case and have found an adhesive contribution similar to the three-dimensional one. We have not carried out a detailed analysis yet, but the same collapse is present in this case, thus indicating a behavior qualitatively similar to the one shown here, except that we cannot say anything on the existence of a solid–solid transition. These results are in perfect qualitative agreement with recent simulations.[48]

## APPENDIX

Let $f(u)$ be an arbitrary function of a single variable $u$. Then $\int_{u-\epsilon/2}^{u+\epsilon/2} f(t)\,dt = \epsilon f(u) + O(\epsilon^3)$, and $\frac{1}{2}[f(u+\epsilon/2) + f(u-\epsilon/2)] = f(u) + (\epsilon^2/8)f''(u) + O(\epsilon^4)$. Accordingly, if $f(\mathbf{r})$ is an arbitrary function of $\mathbf{r}$, from the definitions (4) and the expansions above, it follows $f*\omega_2^{(0)} = f + (\epsilon^2/8)\nabla^2 f + O(\epsilon^4)$ and $f*\omega_2^{(\alpha)} = \epsilon^\alpha f + O(\epsilon^{\alpha+2})$, the latter for $\alpha = 3$ or any vector component of $\alpha = 2$ and 1. Then

$$n_0 = \xi_0 \epsilon^{-2} + \xi_1 \epsilon^{-1} + \{\bar{n}_0 + \xi_2 + \tfrac{1}{8}\nabla^2 \xi_0\} + O(\epsilon),$$

$$\mathbf{n}_1 = \xi_0 \mathbf{u}\epsilon^{-1} + \{\xi_1 \mathbf{u} + \bar{\mathbf{n}}_1\} + O(\epsilon),$$

$$\mathbf{n}_2 = \{\xi_0 \mathbf{u} + \bar{\mathbf{n}}_2\} + \xi_1 \mathbf{u}\epsilon + O(\epsilon^2),$$

$$n_3 = \bar{n}_3 + \epsilon \xi_0 + \epsilon^2 \xi_1 + \epsilon^3 \xi_2 + O(\epsilon^4),$$

where $\mathbf{u} \equiv (1,1,1)$, $\bar{n}_\alpha \equiv \eta * \omega_1^{(\alpha)}$, and the functions $\xi_i$ are defined in (38).

Using these expansions we can obtain

$$\sum_\alpha \frac{\partial \Phi}{\partial n_\alpha} * \omega_2^{(\alpha)} = -\ln(1-\bar{n}_3) + \frac{8\xi_0 + \bar{n}_2}{1-\bar{n}_3}\epsilon + O(\epsilon^2).$$

On the other hand, $\ln\xi = \ln\xi_0 + (\xi_1/\xi_0)\epsilon + O(\epsilon^2)$, hence (37) implies

$$\xi_0 = z(1-\bar{n}_3), \tag{A1}$$

$$\xi_1 = -z\bar{n}_2 - 8z^2(1-\bar{n}_3). \tag{A2}$$

We can now proceed to expand $\Upsilon$ itself:

$$\Phi + \epsilon^{-2}\xi[\ln(\xi/z) - 1]$$

$$= -z(1 - \bar{n}_3)\epsilon^{-2} + \{z\bar{n}_2 + 4z^2(1 - \bar{n}_3)\}\epsilon^{-1}$$

$$+ \left\{ z\bar{n}_1 - 6z^2\bar{n}_2 - \frac{55}{2}z^3(1 - \bar{n}_3) \right.$$

$$+ \left. \frac{z}{8}\nabla \cdot [\ln(1 - \bar{n}_3)\nabla\bar{n}_3] + \bar{\Phi} + \Phi^{ad} \right\} + O(\epsilon).$$

where $\Phi^{ad}$ is defined in Eq. (40) and $\bar{\Phi}$ is given by (5) with the $n_\alpha$ replaced by $\bar{n}_\alpha$ (i.e., it is the excess free-energy functional of the one-component PHC fluid). Expression (39) follows from this equation if we notice that $\int \nabla \cdot [\ln(1 - \bar{n}_3)\nabla\bar{n}_3] = 0$, which holds if the density is constant at the boundaries or if it is a periodic function.

[1] J. A. Cuesta and Y. Martínez-Ratón, J. Chem. Phys. **107**, 6379 (1997).

[2] J. A. Cuesta and Y. Martínez-Ratón, Phys. Rev. Lett. **78**, 3681 (1997).

[3] R. W. Zwanzig, J. Chem. Phys. **24**, 855 (1956).

[4] W. G. Hoover and A. G. de Rocco, J. Chem. Phys. **36**, 3141 (1962).

[5] W. G. Hoover and J. C. Poirier, J. Chem. Phys. **38**, 327 (1963).

[6] F. van Swol and L. V. Woodcock, Mol. Simul. **1**, 95 (1987).

[7] E. A. Jagla, Phys. Rev. E **58**, 4701 (1998).

[8] T. R. Kirkpatrick, J. Chem. Phys. **85**, 3515 (1986).

[9] M. Dijkstra and D. Frenkel, Phys. Rev. Lett. **72**, 298 (1994); M. Dijkstra, D. Frenkel and J.-P. Hansen, J. Chem. Phys. **101**, 3179 (1994).

[10] J. A. Cuesta, Phys. Rev. Lett. **76**, 3742 (1996).

[11] J. S. Rowlinson and F. Swinton, *Liquids and Liquid Mixtures* (Butterworths Scientific, London, 1982).

[12] T. W. Melnyk and B. L. Sawford, Mol. Phys. **29**, 891 (1975).

[13] D. J. Adams and I. R. McDonald, J. Chem. Phys. **63**, 1900 (1975).

[14] V. Ehrenberg, H. M. Schaink, and C. Hoheisel, Physica A **169**, 365 (1990).

[15] H.-O. Carmesin, H. L. Frisch, and J. K. Percus, J. Stat. Phys. **63**, 791 (1991).

[16] J. L. Lebowitz, Phys. Rev. A **133**, 895 (1964).

[17] J. L. Lebowitz and J. S. Rowlinson, J. Chem. Phys. **41**, 133 (1964).

[18] T. Biben and J.-P. Hansen, Phys. Rev. Lett. **66**, 2215 (1991).

[19] H. N. W. Lekkerkerker and A. Stroobants, Physica A **195**, 387 (1993).

[20] Y. Rosenfeld, Phys. Rev. Lett. **72**, 3831 (1994); J. Phys. Chem. **99**, 2857 (1995).

[21] J. S. van Duijneveldt, A. W. Heinen, and H. N. W. Lekkerkerker, Europhys. Lett. **21**, 369 (1993).

[22] P. D. Kaplan, J. L. Rouke, A. G. Yodh, and D. J. Pine, Phys. Rev. Lett. **72**, 582 (1994); A. D. Dinsmore, A. G. Yodh, and D. J. Pine, Phys. Rev. E **52**, 4045 (1995).

[23] U. Steiner, A. Meller, and J. Stavans, Phys. Rev. Lett. **74**, 4750 (1995).

[24] A. Imhof and J. K. G. Dhont, Phys. Rev. Lett. **75**, 1662 (1995).

[25] W. C. K. Poon and P. B. Warren, Europhys. Lett. **28**, 513 (1994).

[26] C. Caccamo and G. Pellicane, Physica A **235**, 149 (1997).

[27] P. H. Fries and J.-P. Hansen, Mol. Phys. **48**, 891 (1983).

[28] G. Jackson, J. S. Rowlinson, and F. van Swol, J. Phys. Chem. **91**, 4907 (1987).

[29] A. Buhot and W. Krauth, Phys. Rev. Lett. **80**, 3787 (1998).

[30] Y. Mao, M. E. Cates, and H. N. W. Lekkerkerker, Physica A **222**, 10 (1995).

[31] T. Biben, P. Bladon, and D. Frenkel, J. Phys.: Condens. Matter **8**, 10799 (1996).

[32] N. García-Almarza and E. Enciso, Phys. Rev. E **59**, 4426 (1999).

[33] M. Dijkstra, R. van Roij, and R. Evans, Phys. Rev. Lett. **81**, 2268 (1998).

[34] P. Bolhuis and D. Frenkel, Phys. Rev. Lett. **72**, 2211 (1994); P. Bolhuis, M. Haagen, and D. Frenkel, Phys. Rev. E **50**, 4880 (1994).

[35] C. F. Tejero, A. Daanoun, H. N. W. Lekkerkerker, and M. Baus, Phys. Rev. Lett. **73**, 752 (1994); Phys. Rev. E **51**, 558 (1995).

[36] M. Dijkstra, R. van Roij, and R. Evans, Phys. Rev. Lett. **82**, 117 (1999).

[37] T. Biben and J.-P. Hansen, Europhys. Lett. **12**, 347 (1990).

[38] Y. Heno and C. Regnaut, J. Chem. Phys. **95**, 9204 (1991).

[39] Y. Martínez-Ratón and J. A. Cuesta, Phys. Rev. E **58**, R4080 (1998).

[40] R. Evans in *Inhomogeneous Fluids*, edited by D. Henderson (Dekker, New York, 1992).

[41] W. H. Press, S. A. Teukolsky, W. T. Vetterling, and B. P. Flannery, *Numerical Recipes*, 2nd ed. (Cambridge University, New York, 1992).

[42] Notice that a FMT functional has no particular difficulties to account for vacancies in a crystal lattice, in contrast to what happens for most classical functionals. See Ref. 40 for a more detailed discussion on this matter.

[43] H. B. Callen, *Thermodynamics* (Wiley, New York, 1960).

[44] G. Stell, J. Stat. Phys. **63**, 1203 (1991).

[45] C. F. Tejero and M. Baus, Phys. Rev. E **48**, 3793 (1993).

[46] D. Frenkel (private communication).

[47] R. P. Sear, Europhys. Lett. **44**, 531 (1998).

[48] A. Buhot and W. Krauth, Phys. Rev. E **59**, 2939 (1999).